GIANT DIPOLE RESONANCE IN HOT NUCLEI

N. VINH MAU

Division de Physique Théorique[1], Institut de Physique Nucléaire,
F-91406 , Orsay Cedex, France

Lectures given at the II Taps workshop at Guardamar(Spain)
May 31-June 5,1993

IPNO/TH 93.39

[1] Unité de Recherche des Universités Paris XI et Paris VI associée au C.N.R.S

In cold nuclei, giant resonances built on ground state are well known to come from collective effects due to strong interactions between individual nucleons and are well described by RPA.When studying giant resonances built on an excited state of the nucleus at a finite temperature T, three questions arise: - how long such collective effects occur in a nucleus when T increases? -how the properties of the giant resonances vary when the temperature increases? -how the study of giant resonances in hot nuclei can give us information on the structure of the nucleus in a highly excited state?

The tentative answers to these questions in the case of the giant dipole resonance are the object of my talks. In the first part, some of the experimental results will be rewieved and in the second one, their theoretical interpretation will be discussed.

I.EXPERIMENTAL DATA.

The giant dipole resonance (GDR) built on an excited state of the nucleus has been seen for the first time in 1981 in Berkeley[1] in deeply inelastic products from nucleus-nucleus collisions but in most of the experiments, the GDR is studied by measuring the spectrum of high energy γ -rays emitted by the compound nucleus formed in a nucleus-nucleus collision. The statistical nature of this γ -ray emission, or equivalently the γ-ray emission by a thermally equilibrated compound nucleus, has been demonstrated in many experiments at low and medium temperatures . For example in one of the first experiments[2], the shape of the γ-ray spectra corresponding to ^{63}Cu*, ^{76}Kr* and ^{96}Cs* formed in two different reactions with projectiles ^{12}C and ^{18}O leading to the same excitation energy and similar spin states are seen to be independent of the entrance channel as shown in Fig.1 for ^{76}Kr*.

A typical γ-ray spectrum measured in such heavy ion collisions is shown in Fig.2 for the case of ^{40}Ar+ ^{70}Ge forming ^{110}Sn at high excitation energy [3]. At the lowest γ energies one has the exponential shape typical of γ-ray emission following particle evaporation.

At the highest γ-ray energies one sees the nucleon-nucleon bremsstrahlung contribution due to γ-rays emitted in the early stages of the collision before equilibration of the compound nucleus and due to nucleon-nucleon collisions. This part of the spectrum varies also exponentially with the γ-ray energy. This contribution is important only in high energy collisions. In between, one sees an excess of γ-rays of energy $\simeq$15-20 MeV which is approximately the same for all systems and characteristic of a γ-ray coming from the deexcitation of a giant dipole resonance.

To analyse such a spectrum the nucleon-nucleon bremsstrahlung contribution which is not of statistical nature is first subtracted from the experimental spectrum. Then the spectrum

is analysed in terms of the statistical model. The decay rate for the emission of a γ-ray by a nucleus in state i with energy E_i and spin I_i desexciting to a state f with energy E_f and spin I_f is given in the statistical model as:

$$R_\gamma d\gamma = \frac{\rho(E_f, I_f)}{\rho(E_i, I_i)} f_D(E_\gamma)\, d\gamma \tag{1}$$

where $\rho(E, I)$ is the level density at energy E and spin I and $f_D(E_\gamma)$ is the GDR strength function which is assumed to have the same Lorentzian shape as for the GDR built on the ground state. Then one writes:

$$f_D(E_\gamma) = \frac{4e^2}{3\pi(\hbar c)(mc^2)} S_D \frac{NZ}{A} \frac{\Gamma_D E_\gamma^4}{(E_\gamma^2 - E_D^2)^2 + \Gamma_D^2 E_\gamma^2} \tag{2}$$

where S_D is the dipole strength in terms of the classical sum rule, E_D and Γ_D the GDR energy and width respectively.

The strength, eq.2, has been written for a single peak. For deformed nuclei or when one includes a possible contribution of the giant quadrupole resonance, the single Lorentzian is simply replaced by the sum of several Lorentzians.

The level density of eq.1 depends upon the Bethe level density parameter a. At low excitation energy $a \simeq A/8$ but it has been found [4] that a decreases to the Fermi gas value $a \simeq A/13$ for temperatures $T > 3 - 4$ MeV. This temperature dependence of a has been taken into account in some of the analyses of experimental spectra but does not modify strongly the fitted values of E_D and Γ_D.

These expressions, eqs.1-2, are put in a CASCADE code where E_D, Γ_D and S_D are adjusted in order to fit the experimental spectrum, if necessary subtracted from the bremsstrahlung contribution.

The result of such an analysis is shown in Figs.2 and 3 for ^{40}Ar + ^{70}Ge $\rightarrow$ ^{110}Sn at E_x=230 MeV. In Fig.2 is plotted the total experimental and fitted spectra and in Fig.3 the "divided" spectrum: to allow a plot in linear scale one divides the experimental spectrum by the exponential $\exp(-\alpha E_\gamma)$ which reproduces the low energy part of the spectrum. The sensitivity to the GDR parameters and to the level density parameter a is shown in Fig.3. One sees that there is a strong sensitivity to Γ_D but a weak sensitivity to a. A good fit of the experimental spectrum corresponds for both cases, a varying or not with temperature, to E_D=16 MeV and Γ_D= 13 MeV. The energy is close to the ground state GDR energy, even though sligthly lower, but the width is about twice what it is at T=0. These features are common to all experiments, as we shall see below.

In the recent years, the angular distribution of the emitted γ-rays has been also measured. These measurements bring more information about the type of reaction and about the structure of the GDR and therefore about the properties of the hot compound nucleus. Indeed one knows that: a. if the γ-ray emission is purely stastistical, therefore if a thermally equilibrated compound nucleus has been formed, the angular distribution is symmetric about θ_γ=90^0 (θ_γ is the angle between the γ-ray and the beam direction)-b. if the compound nucleus is spherical, it should be nearly isotropic. If it is deformed, one should see an anisotropy which depends on the type of deformation. Let's write the differential cross section as:

$$\frac{d^2\sigma(E_\gamma,\theta_\gamma)}{d\Omega_\gamma dE_\gamma} = A_0(E_\gamma)[1 + a_1(E_\gamma)P_1(cos\theta_\gamma) + a_2(E_\gamma)P_2(cos\theta_\gamma)] \quad (3)$$

E_γ and θ_γ are expressed in the center of mass frame. The symmetry about θ_γ=90^0 means that a_1=0 while $a_2 \neq$0 gives an indication of the deformation of the compound nucleus. On Fig.4 are given the coefficients a_1 and a_2 extracted from angular distribution as a function of the γ-ray energy in the case of ^{18}O + ^{27}Al at 44.9 and 72.5 MeV and ^{12}C + ^{27}Al at 62.37 MeV [6]. In all cases a_1 is zero to a good precision, which is verified for all studied systems showing the statistical nature of the γ-ray emission while a_2 seems slightly negative for E_γ <20 MeV, compatible with zero above, what is an indication that the compound nucleus is deformed with an oblate shape.

A general review of all experiments can be found in ref.[5]. In this talk it is impossible to make such a complete review. Therefore I have made a choice such that all the most typical effects are well illustrated and such that they cover the domain from light to heavy compound systems including spherical and deformed nuclei. Indeed when the temperature is finite and large enough all nuclei are opened shell nuclei, shell effects or deformation effects are expected to desappear and all nuclei are expected to behave the same way. However as we shall see the situation is not that simple.

In the fusion of two nuclei, not only excitation energy or equivalently temperature is transferred to the compound nucleus but also angular momentum. When the collision energy increases, both temperature and average transferred angular momentum increase. Theoretically the effects of these two variables can be separated while experimental results are the result of both. Therefore to understand better each process it is useful to look for experiments or to compare different experiments such that one is able to eliminate, or nearly eliminate, the effects due to one of these. Therefore our choice of the discussed experimental data has been, for each type of systems, guided by this aim.

Compound Nucleus	E_{xi} (MeV)	I_f ($\hbar$)	E_{rot} (MeV)	E_{xf} (MeV)	T_f (MeV)	S_G	E_G (MeV)	Γ_G (MeV)
^{39}K	60.	16.	18.7	13.9	1.69	0.86±0.06	17.±0.1	13.4±0.4
	50.	13.	12.5	14.3	1.71	0.77±0.05	16.8±0.1	11.6±0.4
	40.	8.	5.	14.9	1.75	0.89±0.11	16.4±0.1	10.5±0.3
^{40}K	46.3	9.5	6.6	17.8	1.88	1.33±0.09	17.2±0.1	12.1±0.4
^{42}Ca	50.2	12.5	10.3	16.7	1.78	1.17±0.08	17.1±0.1	11.9±0.4
	40.2	8.	4.4	16.5	1.77	1.19±0.08	17.7±0.1	11.6 ±0.3
^{45}Sc	66.6	18.5	19.6	17.8	1.78	0.97±0.07	16.3±0.1	14.7±0.5
	60.	16.	14.8	17.7	1.77	0.87±0.06	16.1±0.1	12.4±0.4
	50.	13.	9.9	16.8	1.73	0.76±0.05	16.1±0.1	12.1±0.4
	42.	8.	3.9	16.1	1.69	0.75±0.05	17.±0.1	11.6±0.3

Table 1: *Reaction parameters and fitted GDR parameters. Taken from ref[6].*

A) *Nuclei in the mass region A=39-45*

An extensive study of ^{39}K,^{40}K, ^{42}Ca and ^{45}Sc formed by bombarding ^{27}Al with ^{12}C, ^{13}C, ^{15}N and ^{18}O ions of different energies has been achieved [6]. All these nuclei are spherical or nearly spherical in their ground state. An interesting feature of these experiments is that for all systems and all incident energies the temperature is nearly the same $T \simeq 1.7 - 1.8$ MeV, then the results will give direct information on the effect of the average transferred spin which takes values from 8 to 18.5 $\hbar$ as seen in the table 1 where are given the characteristics of the reactions and the fitted values of E_D and Γ_D. E_{xi} is the bombarding energy, E_{rot} the rotationnal energy due to the final spin I_f of the compound nucleus and E_{xf} the excitation energy of the compound nucleus in its final state (equilibrium state) which determines the temperature and is given by:

$$E_{xf} = E_{xi} - E_{rot} - E_D = aT_f^2 \tag{4}$$

with:

$$E_{rot} = \frac{1}{2\mathcal{I}} I(I+1) \tag{5}$$

where $\mathcal{I}$ is the moment of inertia of the compound nucleus. In Fig.5 the GDR strength, energy and width are plotted as a function of spin. One sees that:

a) in this analysis there is no evidence for a deformation of these hot nuclei: the γ-ray spectra are all well fitted by a single Lorentzian.

b) the strength S_D is constant and the same that at T =0

c) the energy E_D does not vary but is smaller than at $T = I = 0$

d) the width Γ_D is much larger than at $T = I = 0$ and increases smoothly with I. However if one extrapolates the measured points to lower I one gets a still much larger value than at $T = 0$. This suggests an important effect on the width due to temperature only.

e) all results for the different nuclei are similar what indicates that at $T \simeq 1.8$ MeV shell effects are not important.

In Fig.4, one has seen already the result of the measurement of the coefficients a_1 and a_2 of eq.3 as a function of E_γ . The fluctuations in a_1 and a_2 for E_γ <10 MeV may come from non statistical processes, then only values for E_γ >10 MeV are considered. In this domain a_1 is compatible with zero while a_2 is slightly negative for E_γ <20 MeV, then close to zero, what is an indication for an oblate deformation of the compound nuclei sometimes interpreted as due to the rotation of the nucleus induced by the spin, even though it is not observed from the spectra analysis. However, the upper and lower curves correspond to very different average spins (8 and 18.5 $\hbar$ respectively) while the a_2 coefficients are very similar in the two cases, suggesting that an interpretation of this apparent deformation as due to spin only is probably not sufficient.

B) *The ^{63}Cu nucleus*

The Seattle group[7] has studied the nucleus of ^{63}Cu formed at different excitation energies and different spins in four reactions: ^{4}He+ ^{59}Co, ^{6}Li+^{57}Fe, ^{12}C+^{51}V and ^{18}O+^{45}Sc. The GDR built on ground state presents a double peak which is due to isospin splitting rather than to a deformation splitting. The table 2 gives the reaction parameters and the GDR parameters fitted with a single Lorentzian on the γ-ray spectra shown in Fig.6. The fits in terms of statistical model are very good for the upper curves of Fig.6 corresponding to ^{18}O and ^{12}C projectiles. For ^{4}He and ^{6}Li projectiles at higher bombarding energies there is a deviation in the highest part of the spectra showing the presence of non statistical effects. This is not surprising for such light projectiles and the corresponding fitted GDR parameters should be taken with some care. All spectra are well fitted with a single Lorentzian showing no deformation. The fitted GDR strength, energy and width are shown in Fig.7 as a function of the final energy E_{xf} defined by eqs.4-5. The strength and energy do not vary with temperature and are close to their ground state values while the width increases regularly between E_{xf}=0 (if one excludes the two first points corresponding to α projectile) and the highest values of E_{xf}. Higher bombarding energies correspond to higher temperatures but also to higher spins as seen in the table 2 and it is interesting to plot the results as a function of spin. Such plots show that the GDR strength and energy are independent of average spins. In Fig.8 a two dimensional plot of the GDR width as a function of the square of the temperature and the grazing angular momentum l_0 (related

Entrance channel	E_{xi} (MeV)	E_{xf} (MeV)	T_f (MeV)	I_f ($\hbar$)	S_G	E_G (MeV)	Γ_G (MeV)
$^{16}O+^{45}Sc$	77.4	29.2	1.93	22.	0.90±0.10	16.4±0.3	10.6±0.6
	61.6	27.1	1.86	15.	0.99±0.10	16.3±0.3	9.9±0.5
	52.2	24.6	1.77	8.5	1.10±0.07	16.5±0.4	9.6±0.4
$^{12}C+^{51}V$	65.7	23.2	1.72	20.5	1.07±0.10	17.0±0.3	10.5±0.5
	52.2	19.2	1.56	16.	0.67±0.07	16.8±0.3	9.3±0.3
	39.5	16.6	1.45	9.5	0.97±0.05	16.7±0.3	7.7±0.2
	34.7	12.9	1.28	4.5	1.37±0.12	17.1±0.5	8.1±0.6
$^{6}Li+^{57}Fe$	52.	23.7	1.73	10.	0.87±0.07	17.6±0.4	10.2±0.3
	39.5	17.7	1.5	7.5	0.80±0.07	17.1±0.5	8.8±0.3
	32.	12.	1.23	3.	0.74±0.10	16.5±0.6	8.2±0.8
$^{4}He+^{59}Co$	32.4	11.1	1.19	7.5	2.09±0.2	17.2±1.2	7.9±0.3
	28.1	7.3	0.96	7.8	0.87±0.08	17.4±0.4	7.5±0.4
	22.5	4.3	0.74	5.5	1.25±0.08	17.1±0.1	7.8±0.6

Table 2: *Extracted parameters of the GDR built on highly excited states of ^{63}Cu. The cases $^{6}Li+^{57}Fe(52MeV)$ and $^{4}He+^{59}Co(32.4\ MeV)$ are contamined by non statistical contributions. Taken from ref[7].*

to the final spin) is presented. It is seen that the width varies with both but the temperature dependence seems to be dominant.

C) *Nuclei with A=90-100*

The compound nuclei ^{90}Zr, ^{92}Mo, ^{96}Mo and ^{100}Mo have been studied by different groups[8, 9, 10, 11] but I will discuss only the results of the Seattle group[10] who compare the results obtained for the nuclei ^{92}Mo and ^{100}Mo which in their ground state are of different nature: the ^{92}Mo is a very soft, nearly spherical nucleus while the ^{100}Mo is a strong vibrator. Therefore this comparison gives very interesting information on the role and evolution of the structure of nuclei when the temperature and the transferred spin increase.

The compound nuclei of ^{92}Mo and ^{100}Mo are formed in two different reactions, $^{16}O+^{76}Se$ and $^{18}O+\ ^{82}Se$ respectively at different bombarding energies (50 and 72.2 MeV for ^{16}O and 49.1, 63.4 and 72.8 MeV for ^{18}O). They correspond for the two nuclei and the two first energies to the same temperature as can be seen in table 3. Therefore one can hope to extract from a direct comparison of the results the role of the structure of the nuclei in their ground state in the evolution of the nuclear properties at finite temperature.

Compound nucleus	Entrance channel	E_{lab} (MeV)	l_0 ($\hbar$)	E_{xi} (MeV)	T_f (MeV)	I_f ($\hbar$)
^{92}Mo	^{16}O+^{76}Se	50.	13.5	43.1	1.35	9.
		72.2	29.5	66.5	1.45	19.5
^{100}Mo	^{18}O+^{82}Se	49.1	14.	48.1	1.35	9.3
		63.4	29.5	59.8	1.45	19.5
		72.8	36.3	67.5	1.5	24.

Table 3: *Characteristics of the compound nuclear states populated in $^{16}O+^{76}Se$ and $^{18}O+^{82}Se$. Taken from ref[10].*

Compound nucleus	E_{xi} (MeV)	$\overline{E}$ (MeV)	E_2/E_1	S_1+S_2	Γ_1 (MeV)	Γ_2 (MeV)	$\overline{\Gamma}$ (MeV)
^{92}Mo	48.1	16.67±0.28	1.21±0.06	0.90±0.05	5.52±0.52	6.87±2.36	7.63±0.10
	66.5	16.58±0.15	1.23±0.03	0.90±0.05	4.68±0.84	7.31±1.17	8.60±0.20
^{100}Mo	48.1	16.38±0.47	1.22±0.36	1.63±0.28	6.70±4.36	11.48±2.70	9.79±0.20
	59.8	16.17±0.14	1.25±0.03	1.10±0.03	7.20±0.26	9.91±1.04	9.9±0.20
	67.5	15.96±0.24	1.30±0.02	1.03±0.03	7.16±0.48	8.19±1.61	10.06±0.20

Table 4: *The fitted GDR parameters for ^{92}Mo and ^{100}Mo. Taken from ref[10].*

While for the two nuclei the GDR built on the ground state is well described by a single Lorentzian, in these experiments at finite temperature a better fit of the γ-ray spectra is obtained in both nuclei with the sum of two Lorentzians as shown in Fig.9.

The ratio of the energies of the two peaks are reproduced in table 5 as well as the mean energy $\overline{E} = (E_1S_1 + E_2S_2)/(S_1 + S_2)$ and the full width at half maximum $\overline{\Gamma}$ calculated numerically from the fitted strength function. In Fig.10 are presented the variation of $\overline{S} = S_1 + S_2$, $\overline{E}$ and $\overline{\Gamma}$ as a function of the square of the temperature for both nuclei. Again the strength and mean energy show no variation and are close to their values at zero temperature. The widths increase with increasing T. In ^{92}Mo the width seems to increase more sharply than in ^{100}Mo but is still lower, showing that at temperatures $T \simeq 1.5$ MeV shell effects are still present. The uncertainties on the fitted ratio S_2/S_1 are too large to allow a determination of the shape, oblate or prolate, of the two nuclei except for ^{100}Mo and E_x=67.5 MeV where the ratio S_2/S_1 suggests an oblate shape. From the energy splitting of the two components fits to the spectra, one may calculate an effective deformation parameter $\beta = 2/3\sqrt{4\pi/5}\ln(E_2/E_1)$. One finds that at T=1.35 Mev

and $I=9\hbar$ $\beta=0.2\pm$ 0.05 and 0.21 ± 0.27 , at $T=1.45$ MeV and $I=19.5$MeV $\beta=0.22\pm$ 0.03 and 0.24 ± 0.03 for ^{92}Mo and ^{100}Mo respectively. These effective values of β are very close in the two isotopes and do not show much sensibility to the spin. This last observation is in agreement with the rotating liquid drop model[12] where the spin induced equilibrium deformation are found to be $\beta \simeq 0.01, 0.05$ for ^{92}Mo at 9 and 19.5 $\hbar$ and 0.04, 0.06 for ^{100}Mo at 19.5 and 24 $\hbar$ respectively[10].These values are much smaller than requested by the fitting of data, suggesting that the broadening of the GDR is mostly related to temperature.

D) *Sn isotopes A=108-114*

Systematic information on the behaviour of the GDR in these isotopes of tin is available over a very broad energy (E_x=50-600MeV) and spin (up to 40$\hbar$) domains [13, 14, 15, 16, 17, 18, 19, 20]. The results are summarised in the Fig.11 [5].At all energies a single Lorentzian fits well the γ-ray spectrum. As in all experiments the strength and energy of the GDR do not vary and are close to that of the GDR built on the ground state. The width increases sharply from 5.8 to 11 MeV about between E_x=0 and 130 MeV but the new result is that there is a saturation of the width which is for E_x >230 MeV independent of E_x. This has been compared with the saturation of the maximum angular momentum that the compound nucleus can sustain without fissioning which is also shown in Fig.11. Indeed the width and maximum spin saturate at about the same excitation energy and it is tempting to make a direct relation between the two and to conclude that the broadening of the GDR is strongly correlated with the spin of the compound nucleus. However such a strong correlation is not confirmed by other experimental measurements as we have seen above. On the other end, in the fusion of two nuclei a wide range of angular momentum are transferred to the compound nucleus so that a direct relation between maximum spin and width is not obvious.

Even though the γ-ray spectra are well fitted with a single Lorentzian, the measured angular distribution shows an a_2 coefficient compatible with a small deformation which increases with increasing spin. This is shown in Fig.12 for ^{110}Sn at E_x = 92 MeV and ^{109}Sn at E_x = 80 MeV where are plotted the average values of $a_2(E_\gamma)$ for 11< E_γ <14 MeV as a function of the average spins corresponding to different spin gates[21]. However changing spin means changing the thermal excitation energy as well, see eq.4, (increasing spin corresponds to decreasing temperature), therefore in the results of Fig.12 temperature and spin effects are very likely mixed up. One also sees that the calculated values of a_2, taking account of shape fluctuations, show very weak spin dependence(we will go back to shape fluctuations in the next section).

A saturation of the GDR width has also been observed in ^{59}Cu [22] where the width at

E_x ≃100 MeV is very close to that at E_x=77.4 MeV. However the measurements have been done at three different energies only. Furthermore for the middle point which is crucial to conclude to a saturation the comparison between the GDR width in ^{59}Cu and ^{63}Cu in the same energy range shows a different behaviour. While at low excitation energy and low spin the GDR widths are similar in the two nuclei and good fits are obtained with a single Lorentzian, the width is much larger in ^{59}Cu at E_x=77.4 MeV and I_{max} =38$\hbar$ in a two-Lorentzians fit than in ^{63}Cu at the same excitation energy and I_{max} =35$\hbar$. In ref.23 this difference is attributed to spin effect in the following way: the maximum values of spin transferred to the compound nuclei appear to be in the angular momentum range where the rotating liquid drop model predicts a shape transition [23]. If one assumes that this "critical"spin is just between the two values 35 and 38$\hbar$ and one forgets that transferred angular momenta are not so well determined and not restricted to their maximum possible values, then one has the explanation for the difference and can conclude to a saturation of the width in ^{59}Cu, corroborating the result in Sn isotopes. However more experimental results and more precise theoretical calculations are needed to confirm or not these results.

A saturation of the width has also been observed recently in ^{136}Xe+^{48}Ti reaction [24] for E_x/A ≥ 1 MeV, in agreement with the tin result.

E) *Heavy, strongly deformed nuclei with A=150-190*

The GDR in these hot nuclei has been studied by several groups [25, 26, 27, 28, 29, 30, 31, 32]. A general result of all the analyses of experiments is that one need several Lorentzians to fit the data, showing a persistency of deformation in these heavy nuclei. Most experiments select events with emission of few neutrons only and select states in narrow angular momentum domains. I will not talk about all these experiment but select those concerning Er and Dy.

In ^{164}Er and ^{166}Er at moderate temperature (T ≃1 MeV) and moderate spin (I < 25$\hbar$) the data correspond to a prolate deformation similar to their deformation at zero temperature with similar widths[26]. At higher excitation energy (E_x ≃ 60 MeV , T ≃ 1.6 MeV for ^{164}Er [25] and E_x ≃ 70MeV, T ≃1.8 MeV for ^{166}Er [29]) and higher spins (up to 60$\hbar$ about) the analysis of results suggests a change from prolate to oblate shape in both nuclei. This is shown in Fig.13 [29] where angular distribution and spectra are shown for three different spin windows in ^{164}Er. The analysis of the data shows also a shift of the GDR centroid energy to lower energy with increasing spin which seems to be mainly caused by a shift of the lower GDR component. This is shown in Fig.14. The same conclusions on shape transition and shift of the centroid GDR energy at high temperature and spin have been observed in ^{151}Dy and ^{156}Dy [30] while at

medium temperature widths and shapes are similar to what they are at zero temperature [32].

The measurements in heavy nuclei of such exclusive spectra where only few reaction channels and narrow spin domains are selected seem to give GDR widths much smaller than those extracted from inclusive spectra and to enhance the sensitivity of the analysis of γ-ray spectra to the GDR parameters as discussed by Atac et al [33] for ^{190}Hg. In this case the width extracted from the inclusive spectrum is about 3 MeV larger than that extracted from exclusive spectrum. If it was a general result it will change greatly our view on the problem and the discussion and interpretation of results, in particular it will modify the apparent deformation found in nuclei which are spherical in their ground state and deduced from the very large measured GDR width.

F) *Saturation of the GDR strength*

A first study of the GDR decay at high excitation energy with ^{40}Ar beams at 15 and 24 MeV/u to produce ^{110}Sn excited up to E_x=600 MeV was made in Grenoble in 1987 [34]. At E_x=320 MeV the spectrum is well reproduced by the statistical model with a dipole strength compatible with 100% of the sum rule but the γ-multiplicity has been found the same at 24 MeV/u than at 15 MeV/u, so about half what it should be following statistical predictions, while the fitted energy and width are the same. This is supported by further studies [35, 36].The respective behaviours of the strength which suddenly decreases to a very small value and of the width which does not increase above 230 MeV excitation energy constitutes a very important information which should be confirmed on other compound systems. Indeed the simplest theoretical explanation of this disappearence of the GDR relies on the expectation of a large spreading of the resonance strength over an increasing number of n particle-n hole ($n \geq 1$) states, leading to a very large width. Consequently one looses the characteristics of a resonance but this explanation is ruled out by the experimental results rewieved above. A different analysis of the experimental γ-ray spectra for nuclei with mass number around 120 at very high excitation energy (up to 600MeV) leads to very different results for the GDR width and strength [37]. The authors take into account that the γ-rays can be emitted all through the evaporation chain and introduce in their CASCADE code a mass and excitation energy dependence of the GDR parameters. They find a very large and strongly increasing width with, for the highest excitation energies , a structureless strength function showing that the GDR peak in the spectrum comes from γ-rays emitted by nuclei with low excitation energy. In their analysis the GDR gradually disappears at $T \simeq 3.5$ MeV due to the excessive broadening. Kasagi et al [38] have recently confirmed this result in a series of measurements for nuclei with mass number $A \simeq 70$, 105 and 130. This new result is in agreement with our previous intuitive statement but in disagreement

with other experimental analyses of data.

At such high collision energies the interpretation of the experimental spectra in terms of statistical model is not so well defined as is clear from the different experimental results and would require further studies. .

To summarise all results presented above, we may say that we have learnt several important features concerning the giant dipole resonance in highly excited nuclei. Namely:

1) the energy of the GDR does not vary with temperature and spin (but generally is slightly lower than that of the ground state GDR) except for strongly deformed heavy nuclei where exclusive measurements have shown a lowering of the lowest GDR component with increasing angular momentum.

2) at low and moderate collision energy, the width increases with excitation energy. High angular momentum contributes to this increase which however seems to be mostly due to temperature.

3) the width is found to saturate for $E_x/A \geq 1$ MeV (T$\simeq$3MeV) but there is still some uncertainty on this result.

4) for light and medium nuclei there is no strong evidence that deformation maintains or appears at finite temperature when the γ-ray spectrum is concerned. However when the γ-ray angular distribution has been measured ,the coefficient a_2 is in favor of a deformation of the hot compound system, always corresponding to oblate shapes.

5) in deformed heavy nuclei (Er and Dy isotopes) one sees a shape transition from prolate to oblate shape at quite low temperature ($T \simeq 1.5$ MeV) but high spin.

6) at high temperatures (T$\simeq$ 4-5 MeV) it is found in some experiments that, while the width does not increase, the GDR strength decreases suddenly suggesting a sudden disappearence of the GDR. However in two recent papers a different analysis of data shows a progressive disappearence of the GDR due to a very large broadening of the resonance.

II. THEORETICAL DESCRIPTION OF THE GDR AT FINITE TEMPERATURE

We are dealing with highly excited nuclei. When the excitation energy is large, the level density is so high that it becomes impossible to describe levels one by one. One uses the methods of statistical mechanics, what introduces a parameter, the temperature, which is related to the excitation energy of the nucleus. In such statistical models, only average properties are determined and fluctuations around these average values can be important. It has been shown by Matsubara that at $T \neq 0$ we may apply the same methods and expansions as known at

T=0. Therefore one may use Hartree Fock approximation and RPA built on Hartree Fock single particle states which, as we know, explain very well the GDR properties at T=0, especially the GDR energy.

The Hartree Fock equations at $T \neq 0$ write as:

$$< i|t|j > + \sum_k < ik|V|jk >_A f_k = \epsilon_i \delta_{ij} \tag{6}$$

f_k, the occupation number of a particle in state k, is given by:

$$f_k = \frac{1}{1 + e^{\beta(\epsilon_k - \mu)}} \tag{7}$$

where β is the inverse of the temperature and μ, the chemical potential, is determined such that $\sum_i f_i = N$, N being the mass number of the nucleus. The index A means that the matrix elements of the two body interaction are antisymmetrised.

If $T \neq 0$, f_k takes values between 0 and 1 and the state k is not fully occupied or unoccupied.

The RPA equations are:

$$(\omega_\nu - \epsilon_i + \epsilon_j) X^\nu_{ij} - \sum_{kl} < il|V|jk >_A (f_l - f_k) X^\nu_{kl} = 0 \tag{8}$$

ω_ν and X^ν_{ij} are the energy and particle-hole amplitude of the RPA state ν respectively. The states i,j... are the Hartree Fock particle states determined previously.

The effect of increasing the temperature is two fold:

1. the number of particle-hole configurations increases .

2. the effective particle-hole interaction decreases because of the factors $f_l - f_k$ which are now smaller than 1.

There is in fact a compensation between the two effects so that the collective structure of the RPA states remains at finite temperature explaining the presence of giant resonances in highly excited nuclei. This can be seen on Figs 15 and 16 for the dipole resonance in $^{40}Ca^*$. In Fig.15 are shown the results of a simple RPA calculation [39]: the particle and hole states were described by harmonic oscillator wave functions and energies and the two body interaction was assumed to have zero range and no density dependence. One sees that the energy of the main peak is roughly independent of temperature but when the temperature increases one gets more peaks around the main peak. This means that the resonance has a width due to Landau damping which increases with temperature due to the spreading of the dipole strength over particle-hole states. This effect would contribute to the increase of the experimental width, even though it is certainly not the only contribution. Moreover as seen on Fig.15, at high temperature,$T \geq 4$

MeV, the spreading is so important that one can hardly say that we have still a resonance. This is in qualitative agreement with the analysis of data by Yoshida et al [37] and Kasagi et al [38]. However this behaviour of the GDR is not confirmed by the results of ref[40] which are represented on Fig.16. They correspond to a fully self-consistent RPA calculation including the continuum states and using a Skyrme interaction. The giant dipole resonance which is already very large at T=0 because of the spreading over several states does not change much between T=0 and T=6 MeV. We notice that both calculations agree to say that the energy of the main peak does not vary with temperature but they disagree on the width behaviour. We note on Fig.16 that the escape width which corresponds to the width of each peak is small and is roughly independent of temperature.

RPA calculations have been performed in deformed nuclei [41, 42, 43] with similar results for the two GDR peaks energies. In refs[41,42], because of pairing correlations which are washed out by temperature at $T \simeq 0.5$ MeV, one sees a lowering of the two peaks of 0.5 MeV about between T=0 and 0.5 MeV. Above the peaks energies stay constant. This effect at very low temperature could explain why in most of the experiments, the GDR energy appears to be slightly smaller at $T \neq 0$ than at T=0. This work shows some other interesting features concerning the spin dependence of the GDR: a small shift of the two peaks energies is obtained between I=0 and $I \simeq 40\hbar$ because of pairing collapse but with no variation above. At high spins there is a transition from prolate to oblate shape as indicated by experiments on strongly deformed nuclei.

For the GDR energy all theoretical calculations agree between them and agree with experiments. Concerning the GDR width the situation is more complicated. Widths are always difficult to calculate. At zero temperature the GDR width is already due to several different processes [44]: the spreading over particle-hole states (Landau damping) contributes for 1 MeV about to the total width, the emission of nucleons leads to an escape width which is always quite small, few hundreds KeV, the spreading over two particle-two hole states gives the main contribution to the total width, several MeV [45, 46]. At finite temperature the same processes can contribute to the GDR width, however following Sagawa and Bertsch[40] the escape width is roughly independent of temperature and a calculation of the spreading over two particle-two hole states [47] shows that its contribution is also independent of temperature then cannot contribute to the increase of the GDR width. For the Landau damping the theoretical results are for now on contradictory. As we saw, in a simple RPA calculation, the Landau damping increases with temperature. This seems also the case in a Vlassov semi classical calculation[48] where however the strong increase of the GDR width comes from a competition between Landau damping and

two body collisions. At the contrary in refs[40,47] the Landau damping appears to have no variation with temperature.

The calculation of spreading widths is always delicate because when the temperature increases the number of 1p-1h or 2p-2h states becomes very large and a truncation of the corresponding subspaces could greatly modify the results. A simple model calculation of the effect of the new p-h configurations appearing at finite temperature avoids any truncation of the p-h subspace[49]. One first divides the p-h subspace in two parts: $\mathcal{E}_0$, the p-h subspace at T=0 and $\Delta\mathcal{E}_T$ the subspace formed of all the new p-h states allowed at a given finite temperature T. The RPA equations are first solved for a given temperature T in the subspace $\mathcal{E}_0$ defining a set of independent phonons q of energy ω_q. Then the effect on these independent phonons of their interactions with the particle-hole pairs of the subspace $\Delta\mathcal{E}_T$ is calculated using the Green functions for imaginary times and frequencies. This problem is analogous to treating the interaction between phonons and electrons and the usual methods of statistical physics can be applied [50]. If $D_q^{(0)}$ is the propagator of the free phonon q, the lowest correction to $D_q^{(0)}$ is given by the diagram represented in Fig.17 leading to the perturbed phonon propagator D_q defined by the equation:

$$D_q(i\omega_n) = D_q^{(0)}(i\omega_n) + D_q^{(0)}(i\omega_n)\Pi_q^{(1)}(i\omega_n)D_q^{(0)}(i\omega_n) \tag{9}$$

where $\Pi_q^{(1)}$ is the lowest order contribution to the mass operator and is given by

$$\Pi_q^{(1)}(i\omega_n) = \sum_{\alpha,\beta\in\Delta\mathcal{E}_T} |V(\alpha\beta:q)|^2 \frac{f_\beta - f_\alpha}{i\omega_n - \epsilon_\alpha + \epsilon_\beta} \tag{10}$$

where $V(\alpha,\beta;q)$ is the interaction between the particle-hole pair $\alpha\beta$ and the free phonon q, f_i is the occupation number of state i defined in eq.7 and $\epsilon_\alpha - \epsilon_\beta$ is the particle-hole pair energy. Assuming that the effect of the diagram of Fig.17 is to change the unperturbed phonon energies into a new set of renormalised energies Ω_q we may write:

$$D_q(i\omega_n) = \frac{2\omega_q}{(i\omega_n)^2 - \Omega_q^2} \tag{11}$$

The renormalised energies according to eq.9 are given by:

$$\Omega_q^2 = \omega_q^2 + 2\omega_q \lim_{\eta\to+0} \sum_{\alpha\beta\in\Delta\mathcal{E}_T} |V(\alpha\beta;q)|^2 \frac{f_\beta - f_\alpha}{\omega_q - \epsilon_\alpha + \epsilon_\beta + i\eta} \tag{12}$$

We see that Ω_q is a complex quantity. Its imaginary part is related to the width Γ of the phonon strength function. To calculate this width one uses a schematic model where all quantities can be calculated analytically in the full subspace $\Delta\mathcal{E}_T$. This model relies on the following assumptions: the particle-hole matrix elements are separable, independent of the p-h states and are fitted on

the energy of the ground state GDR and all particle-hole states of subspace $\Delta\mathcal{E}_T$ have the same mean energy ϵ with a Lorentzian dipole strength distribution of width γ. Within this model the real part of Ω_q is independent of temperature and equal to the phonon energy at T=0 what is in agreement with all more realistic calculations . The width of the phonon strength function represents the contribution of the Landau damping due to the new p-h configurations and gives a measure of the enhancement of the one particle-one hole spreading width. It is shown in Fig.18 as a function of temperature for the GDR in ^{208}Pb . One sees a sharp increase up to T$\simeq$3-4 MeV and above, a smoother variation with little sensitivity to the parameter γ . This reproduces quite well the tendency of experimental data. The Landau damping contribution is in this calculation very large but one should remember that the schematic model always overestimates collective effects. However it seems clear that Landau damping should play a non negligible role in the temperature dependence of the GDR width.

The same calculation has been performed in ^{40}Ca with similar results except that the increase of the Landau damping contribution is not as fast as in ^{208}Pb, as expected.

In highly excited nuclei, several new causes of a damping of the GDR may be invoked but we will mention two of them only in this talk.

In the fusion of two nuclei angular momentum is transferred to the compound nucleus as well as temperature. These transferred spins can be quite high, depending of the bombarding energy and of the fusionning system. High spin means rapid rotation of the nucleus which may induce a deformation of the compound nucleus. If the nucleus is deformed the GDR is splitted into two (or three) peaks and what is seen in the experiments is an average of these peaks with an enhancement of the full width. However as we have seen already, according to the rotating liquid drop model this deformation induced by the spin is weak, too weak to explain the apparent deformation deduced from the enhancement of the experimental width.

Another cause of the width enhancement comes from shape fluctuations. At finite temperature, the energy surfaces are shallower than at $T = 0$, they have no pronounced minimum, therefore the nucleus can explore a large domain of deformations outside the equilibrium one. What is measured experimentally is then the average of such shape fluctuations. The shape fluctuations have been calculated in the literature by two groups: Gallardo et al [51, 52] in a cranked Nilsson model with Strutinsky prescription and by Alhassid et al[53, 54, 55] in a macroscopic model based on Landau theory. For a given nucleus at temperature T with spin I one calculates the free energy which is defined as:

$$F(\epsilon\gamma; IT) = < H > - TS - \bar{\omega}. < \bar{I} > \qquad (13)$$

where ϵ, γ are the deformation parameters, S the entropy of the system and ω the angular velocity. F is minimized with respect to the deformation parameters determining the equilibrium shape. At equilibrium the absorption cross section for a dipole radiation of energy E, $\sigma(E;\epsilon\gamma;IT)$ is then calculated either macroscopically or microscopically. As the free energy has no sharp minimum the nucleus can fluctuate around its equilibrium shape and the experiments measure the average of the cross sections corresponding to the different shapes that the nucleus can explore. This average cross section is given by:

$$\begin{aligned} \sigma(E;IT) &= <\sigma(E;\epsilon\gamma;IT)> \\ &= \frac{\int d\tau\, P(\epsilon\gamma;IT)\,\sigma(E;\epsilon\gamma;IT)}{\int d\tau\, P(\epsilon\gamma;IT)} \end{aligned} \tag{14}$$

where P, the probability that the nucleus has a deformation $\epsilon\gamma$, is:

$$P(\epsilon\gamma;IT) \propto exp(-F(\epsilon\gamma;IT)/T) \tag{15}$$

The volume element $d\tau$ associated to the deformation is chosen as:

$$d\tau = \epsilon\, d\epsilon\, d\gamma \tag{16}$$

by Gallardo et al and as:

$$d\tau = \epsilon^4\, |sin(3\gamma)|\, sin\theta\, d\epsilon\, d\gamma\, d\theta\, d\phi \tag{17}$$

by Alhassid et al. The angles $\theta\,\phi$ define the orientation of the nucleus. This later definition of $d\tau$ includes orientation fluctuations as well as shape fluctuations.

The results of both types of calculations are in qualitative agreement: they both show a large increasing of the GDR width with increasing temperature. This is shown in Fig.19 where the dipole average cross section calculated by Alhassid et al[54] for ^{166}Er and ^{140}Ce which are in their ground state respectively deformed and spherical is plotted for different angular momenta and temperatures . One sees that the width varies very strongly with temperature up to $T \simeq 3$ MeV but above has a much slower temperature dependence. One notices also a relatively weak angular momentum dependence in agreement with most of the analyses of experimental data. In Fig.20 is shown the variation of deformation parameters calculated by Gallardo et al [52] in ^{108}Sn as a function of temperature for different angular momenta. In this figure one sees an interesting feature: for low spins there is a transition from deformed to spherical shape at low temperatures ($\simeq$0.5-1 MeV) while for high spins there is a transition from prolate to oblate shapes as found in experiments for Er or Dy. However the calculated prolate to oblate shape transition appears at lower temperature compared to the data.

As a summary one can say that all theoretical works agree that the GDR energy does not vary with temperature in agreement with all measurements. Concerning the enhancement of the GDR width and its variation with increasing temperature, the theoretical situation is not so clear. However it seems that thermal shape fluctuations play an important role and that the influence of angular momentum is not very strong. Besides this effect, an increase of the Landau damping contribution is suggested by some works but this result is still controversy.

III.CONCLUSIONS.

In these two talks we gave a review of experimental data and theoretical predictions on giant dipole resonance in hot nuclei. This rewiev is not exhaustive and the choice of reported results, experimental and theoretical, may not be completely objective. We are aware that, may be, the discussion of results and their interpretation will not satisfy every one but it is unavoidable since similar experiments, made by different groups, lead sometimes to different interpretation as well as similar calculations lead sometimes to different results. We think that it makes the study of the GDR in highly excited nuclei very exciting and shows that we have still a lot to learn and understand about them and a lot of informations to expect from further studies on the structure of hot nuclear many-body systems and therefore on many-body theory and models at finite temperature.

References

[1] J.O.Newton et al, Phys. Rev. Lett. **46** (1981) 1383 and J.E. Draper et al , Phys. Rev. Lett. **49** (1982) 434

[2] E.F. Garman et al, Phys. Rev. **C28** (1983) 2554

[3] A. Bracco et al, Phys. Rev. Lett. **62** (1989) 2080

[4] G. Nebbia et al, Phys. Lett. **B176** (1986) 20 and B. Natowitz, Nucl. Phys. **A482** (1988) 171c

[5] J.J. Gaardhøje, Annu.Rev.Nucl.Par.Sc. 42 (1992)483

[6] M. Kicinska-Habiour et al, Phys. Rev. **C41**(1990) 2075

[7] M. Kicinska-Habiour et al, Phys. Rev. **C36** (1987) 612

[8] J.H. Gundlach et al, Phys. Rev. Lett. **65** (1990) 2523

[9] T.J. Bowles et al, Phys. Rev. **C24** (1981) 1940

[10] M. Kicinska-Habiour et al, Phys. Rev. **C45** (1992) 569

[11] P. Snover, Nucl. Phys. **A482** (1988) 13c

[12] S. Cohen, F. Plasil and W.J. Swiatecki, Ann. of Phys. (N.Y.) **82** (1974) 557

[13] D.R. Chakrabarty et al, Phys. Rev. **36** (1987) 1886

[14] J.J. Gaardhøje et al, Phys. Rev. Lett. **56** (1986) 1783

[15] J.J. Gaardhøje et al, Phys. Rev. Lett. **53** (1984) 148

[16] A. Bracco et al, Nucl. Phys. **A519** (1990) 47c

[17] A. Bracco et al, Phys. Rev. Lett. **62** (1989)2080

[18] A. Stolk et al, Nucl. Phys. **A505** (1989) 241

[19] A. Stolk et al, Phys. Lett. **B200** (1988) 13

[20] D. Pierroutsakou, PhD Thesis Saclay (1993)

[21] F. Camera et al, Phys. Lett. **B293** (1992) 18

[22] B. Fornal et al, Z. Phys. A340 (1991) 59

[23] G. Viesti et al, Phys. Rev. **C40** (1989) 1570

[24] G. Enders et al, Phys. Rev. Lett. **69** (1992) 249

[25] J.J. Gaardhøje et al, Phys. Rev. Lett. **53** (1984) 148

[26] C.A. Gosset et al, Phys. Rev. Lett. **54** (1985) 1486

[27] D.R. Chacrabarty et al, Phys. Rev. **C37** (1988) 1437

[28] H.M. Bruce et al, Phys. Lett. **215** (1988) 237

[29] P. Thirolf et al, Nucl. Phys. **A482** (1988) 93c

[30] A. Stolk et al, Phys. Rev. **C40** (1989) 2454

[31] J.J. Gaardhøjeet al, Nucl. Phys. **A482**(1988) 121c

[32] R.F. Noormant et al, Phys. Lett. **B292** (1992) 257

[33] A. Atac et al, Phys. Lett. **B252** (1990) 545

[34] J.J. Gaardhøje et al, *Phys. Rev. Lett.* **59** (1987) 1409

[35] N. Herrmann et al, Phys. Rev. Lett. **60** (1988) 1630

[36] J.H. Le Faou et al, Int. Winter Meeting on Nuclear Physics. Bormio Italy (1993)-Prepint Orsay (1993)

[37] K. Yoshida et al, Phys. Lett. **B245** (1990) 7

[38] J. Kasagi et al, Nucl. Phys. **A538** (1992) 585c

[39] D. Vautherin and N. Vinh Mau, Nucl. Phys. **A422** (1984) 140

[40] H. Sagawa and G.F. Bertsch, Phys. Lett. **B146** (1984) 138

[41] P. Ring, L.M. Robledo, J.L. Egido and M. Faber, Nucl. Phys. **A419** (1984) 261

[42] P. Ring, Nucl. Phys. **A482** (1988) 27c

[43] S. Kamerdzhiev and D. Zawischa, Phys. Lett. **275** (1992) 1

[44] G.F. Bertsch, P.F. Bortignon and R.A. Broglia, Rev. Mod. Phys.55 (1983) 287

[45] S. Adachi and S. Yoshida, Nucl. Phys. **A306** (1978) 53

[46] S. Adachi and Nguyen Van Giai, Phys. Lett. **B149** (1984) 447

[47] P.F. Bortignon, R.A. Broglia, G.F. Bertsch and J. Pacheco, Nucl. Phys. **A460** (1986) 149

[48] A. Smerzi,A. Bonasera and M. di Toro, Phys. Rev. **C44** (1991) 1713

[49] N. Vinh Mau, Nucl. Phys. **A548** (1992) 381

[50] A.A. Abrikosov, L.P. Gorkov and I.E. Dzyaloshinski, Methods of quantum field theory in statistical physics (Prentice Hall, Englewood Cliffs, NJ, 1963) and G.H. Mahan, Many particle physics (Plenum,N.Y.,1981)

[51] M. Gallardo et al, Nucl. Phys. **A443** (1985) 415

[52] M. Gallardo, Nucl. Phys. **A482**(1988) 65c

[53] Y. Alhassid et al, Nucl. Phys. **A469** (1987) 205

[54] Y. Alhassid, Nucl. Phys. **A482** (1988) 57c

[55] Y. Alhassid and B. Bush, Nucl. Phys. **A509** (1990) 461

[56] Y. Alhassid et al Nucl. Phys. **A514** (1990) 434

Figure captions.

Fig.1: Gamma ray spectra from the decay of ^{76}Kr* at E_x=53.9, 46.3 and 44 MeV. Circles are $^{18}O+^{58}Ni$ data and crosses are $^{12}C+^{64}Zn$ data. The solid curves are statistical model calculations with the indicated GDR parameters. Taken from ref[2].

Fig.2: The γ-ray spectrum for $^{40}Ar+^{70}Ge$ at 10 MeV/u. The solid curve is the result of statistical model with E_G=16 MeV and Γ_G =13 MeV. The dotted line is the estimated bremsstrahlung contribution and the dashed line the sum of the dotted and solid curves. Taken from ref[3].

Fig.3: γ-ray spectrum of Fig.2 subtracted from the bremsstrahlung contribution and multiplied by $exp(E_\gamma/3.2)$. The curves correspond to statistical model calculations with $a = A/8$, E_G=16 MeV and Γ_G=13 MeV (solid line), Γ_G=11 MeV (dotted line), Γ_G=15 MeV (dashed line) and $a = A/8$ up to E_x=130 MeV and $a = A/12$ from E_x=130 MeV, E_G=16 MeV and Γ_G=13 MeV (dotted-dashed line). Taken from ref[3].

Fig.4: Angular distribution coefficients a_1 and a_2 for reactions $^{12}C+^{27}Al \rightarrow ^{39}K^*$ at E_{lab}=62.7 MeV and $^{18}O+^{27}Al \rightarrow ^{45}Sc^*$ at E_{lab}=44.9 and 72.5 MeV as function of the γ-ray energy. Taken from ref[6].

Fig.5: The fitted GDR parameters as a function of final average spin for ^{39}K (crosses), ^{40}K (triangles), ^{42}Ca (empty squares) and ^{45}Sc (full squares). Taken from ref[6].

Fig.6: γ-ray spectra from the decay of $^{63}Cu^*$ formed in four different reactions. The solid lines are statistical model calculations with the GDR parameters of table 2. Taken from ref[7].

Fig.7: The fitted GDR parameters of ^{63}Cu as a function of final excitation energy above the yrast line. Taken from ref[7].

Fig.8: Two dimensional plot of the extracted GDR width of ^{63}Cu as a function of the square of the temperature and the grazing angular momentum l_0. Taken from ref[7].

Fig.9: γ-ray spectrum from the decay of $^{92}Mo^*$ (left curves) and $^{100}Mo^*$ (right curves). The solid lines correspond to the statistical model calculations with the GDR parameters of table 4. Top curves: the measured spectra. Bottom curves: detailed analysis of the divided spectra. Taken from ref[10].

Fig.10: The fitted GDR average parameters of ^{92}Mo amd ^{100}Mo as a function of the square of the temperature. Taken from ref[10].

Fig.11: The fitted GDR parameters as a function of the excitation energy of the $^{108-112}$Sn compound nuclei. The bottom panel shows the maximum angular momentum transferred to

the compound systems. Dashed lines are the average values of the GDR strength and energy in the cold nuclei. The dotted-dashed curve is a parametrisation of the width increase at low excitation energy. Taken from ref[5].

Fig.12: Average values of the $a_2(E_\gamma)$ coefficients in the interval $11 < E_\gamma < 14$ MeV for ^{109}Sn (open squares) and ^{110}Sn (filled circles). The curves correspond to calculations with (solid and dashed lines) or without (dashed-dotted line) shape fluctuations. Taken from ref[21].

Fig.13: Measured angular distribution coefficient A_2 and γ-ray spectra (multiplied by $\exp(E_\gamma/1.9)$ for the decay of ^{164}Er and corresponding to different spin gates. The solid and dashed curves are statistical model calculations for oblate and prolate shapes respectively. Taken from ref[29].

Fig.14: The fitted GDR centroid (left) and two components (right) of ^{164}Er* as a function of angular momentum. Taken from ref[29].

Fig.15: The RPA dipole strength in ^{40}Ca. Taken from ref[39].

Fig.16: The RPA dipole strength in ^{40}Ca. Taken from ref[40].

Fig.17: The second order diagram included in the phonon propagator of eq.9. The points represent the interaction $V(\alpha\beta;q)$.

Fig.18: The Landau damping contribution to the increase of the GDR width as a function of temperature in ^{208}Pb. The curve corresponds to γ=3 MeV, the crosses to γ=2.5 MeV.

Fig.19: Shapes of the GDR cross section in ^{166}Er (top curves) and ^{140}Ce (bottom curves) at different temperatures and different rotationnal frequencies. ω =0,0.4,0.8 MeV correspond respectively to I=15,30,90$\hbar$ in ^{166}Er and I=10,20,55$\hbar$ in ^{140}Ce. Taken from ref[54].

Fig.20: The deformation parameters ϵ and γ in ^{108}Sn as a function of temperature for different values of angular momentum (given in terms of $\hbar$ besides the curves). Taken from ref[52].

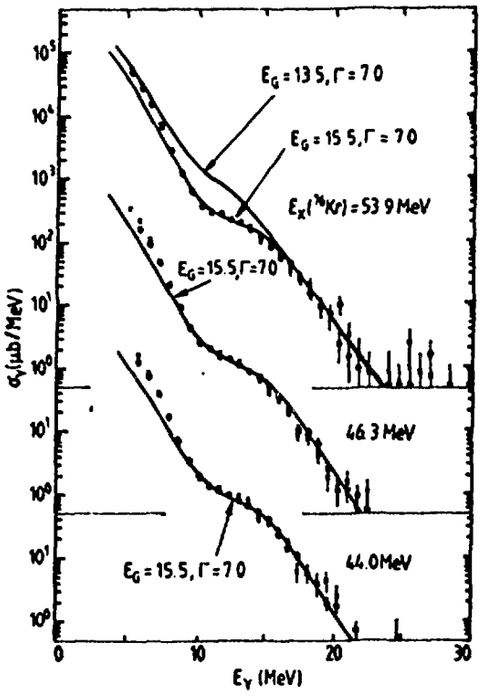

Fig.1

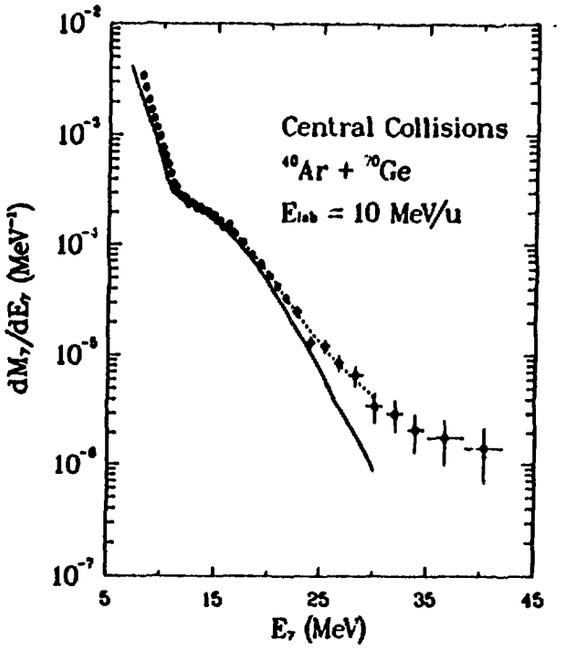

Fig.2

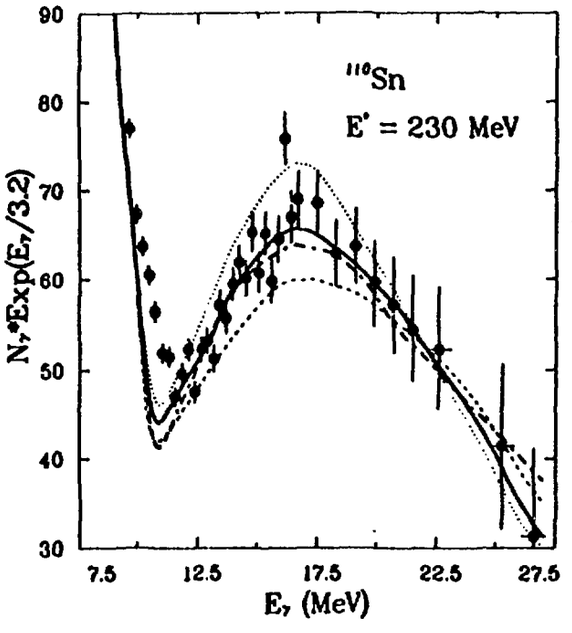

Fig.3

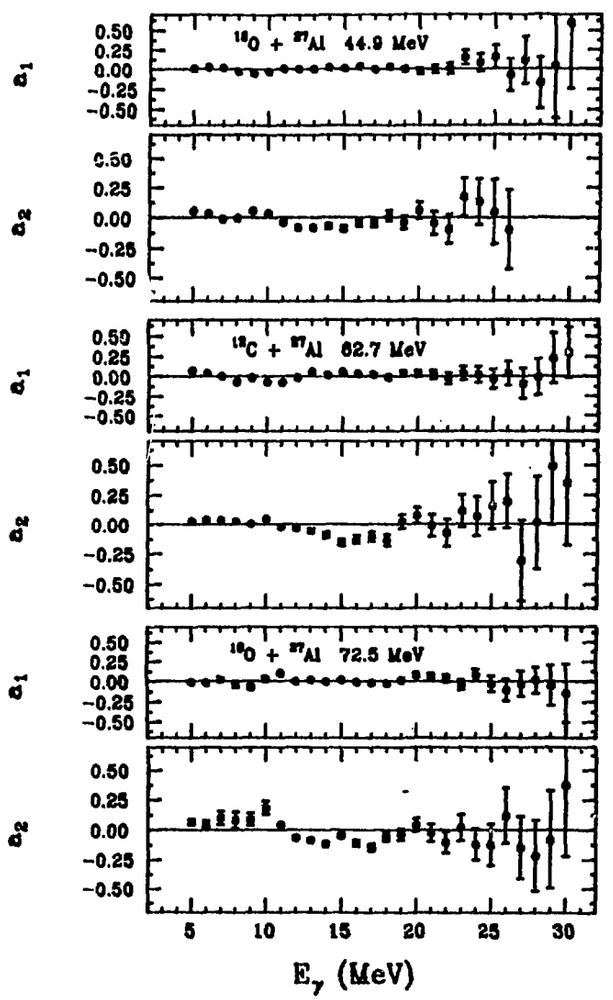
^{16}O + ^{27}Al 44.9 MeV
^{12}C + ^{27}Al 62.7 MeV
^{16}O + ^{27}Al 72.5 MeV
a_1
a_2
0.50
0.25
0.00
−0.25
−0.50
5
10
15
20
25
30
E_γ (MeV)

Fig.4

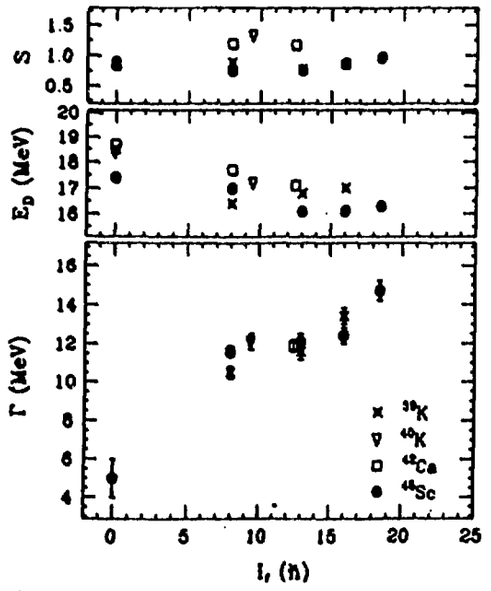

Fig.5

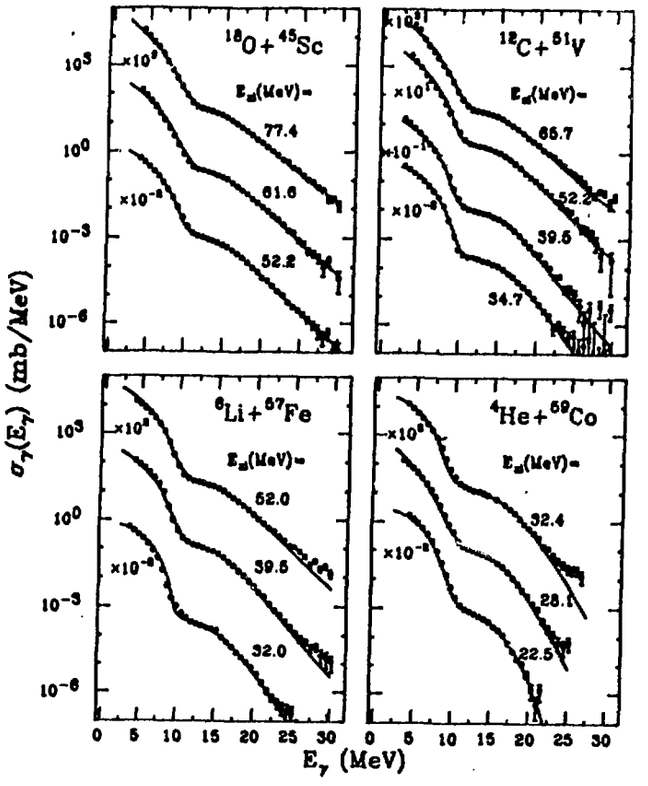

Fig.6

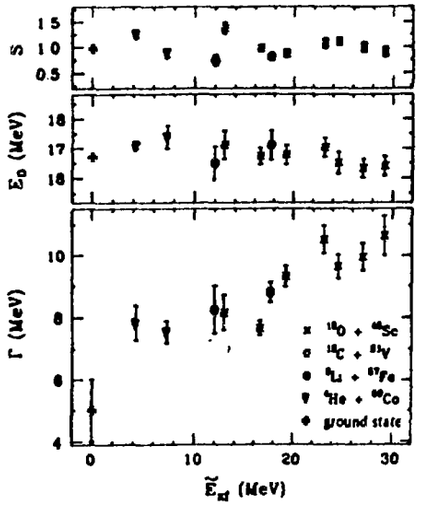

Fig.7

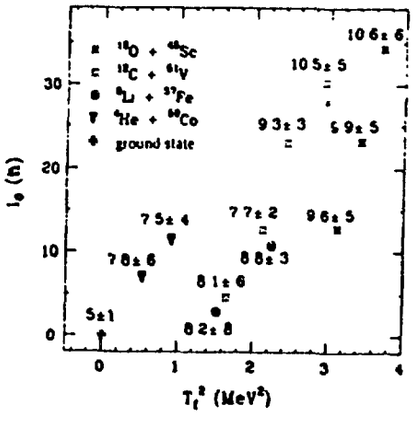

Fig.8

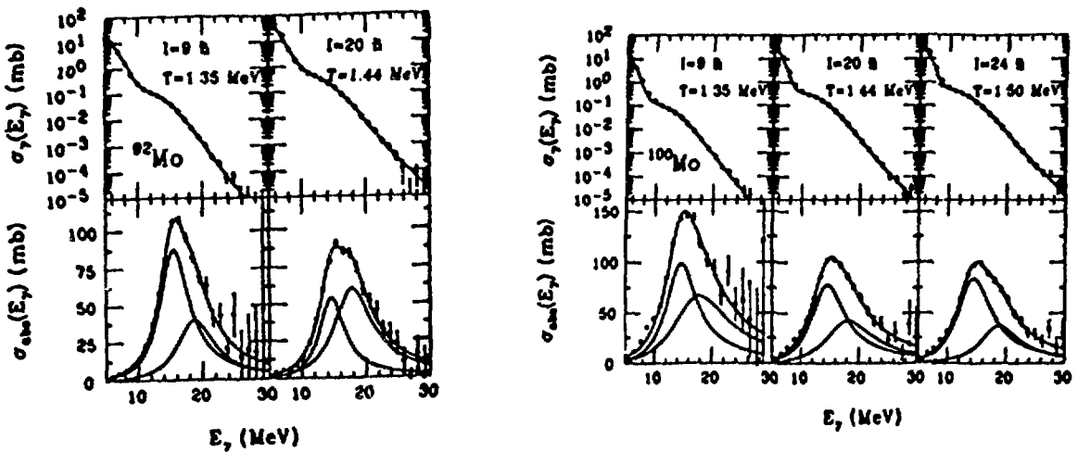
I=9 ħ
T=1.35 MeV
I=20 ħ
T=1.44 MeV
I=24 ħ
T=1.50 MeV
92Mo
100Mo
σγ(Eγ) (mb)
σabs(Eγ) (mb)
Eγ (MeV)

Fig.9

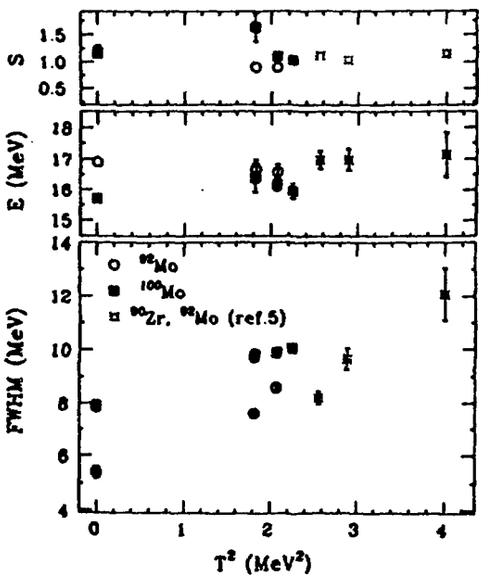
S
E (MeV)
FWHM (MeV)
92Mo
100Mo
90Zr, 92Mo (ref.5)
T² (MeV²)

Fig.10

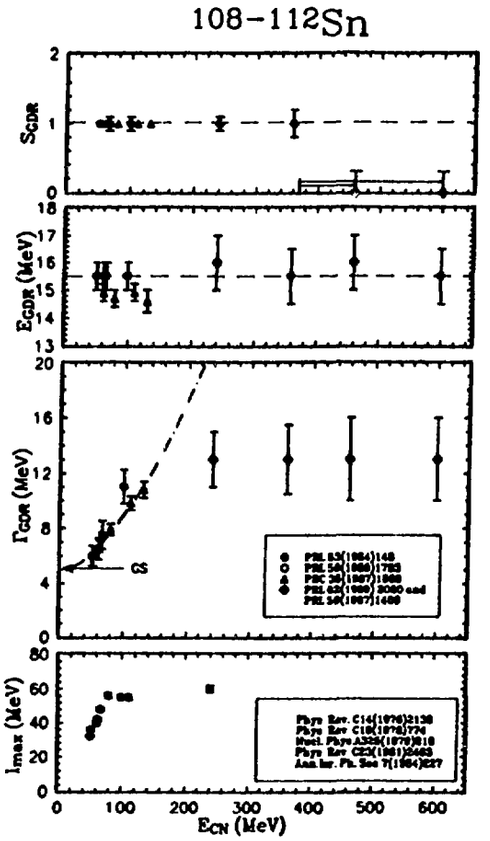
108-112Sn
S_{GDR}
E_{GDR} (MeV)
Γ_{GDR} (MeV)
GS
l_{max} (MeV)
E_{CN} (MeV)

Fig.11

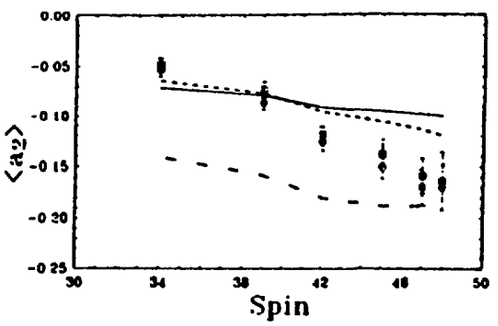
$\langle a_2 \rangle$
Spin

Fig.12

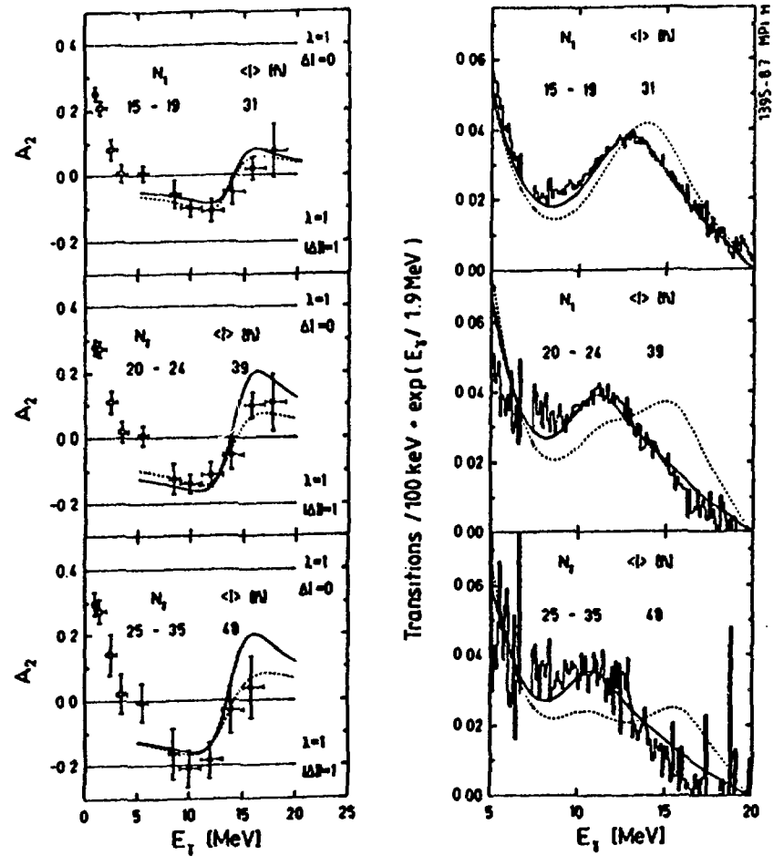
A2
E1 [MeV]
Transitions /100 keV • exp(E1 / 1.9 MeV)
λ=1
Δλ=1
Δl=0
1395-87 MPI H

Fig.13

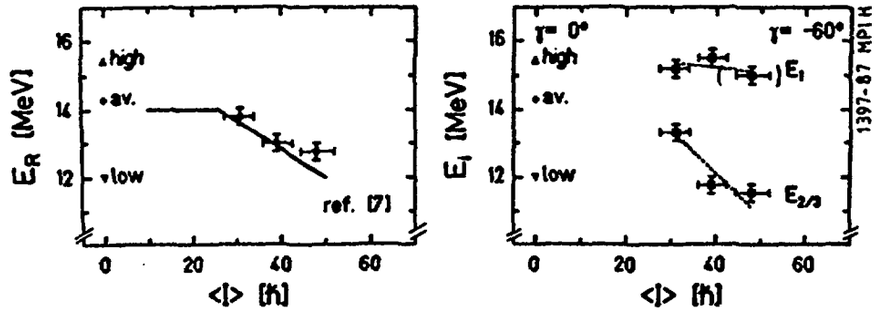
ER [MeV]
E1 [MeV]
<I> [ħ]
high
av.
low
ref. [7]
γ= 0°
γ= -60°
E1
E2/3
1397-87 MPI H

Fig.14

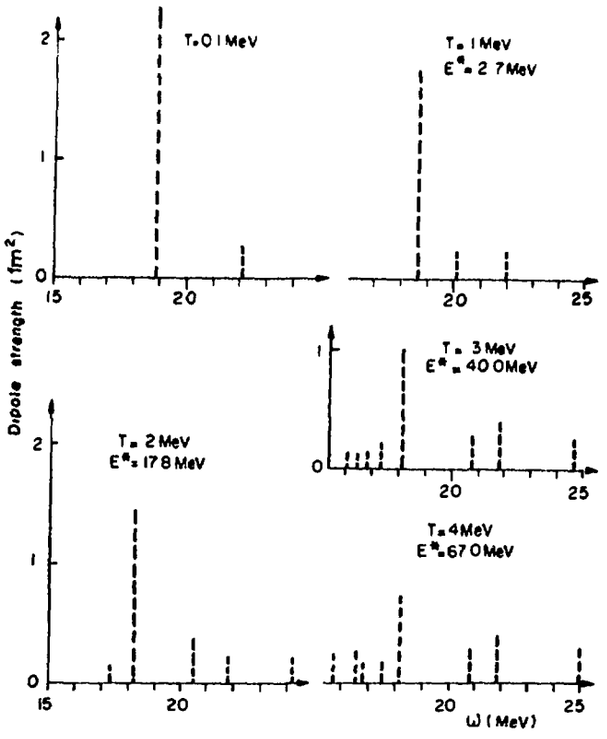
T=0 MeV
T= 1 MeV
E*= 2 7MeV
T= 3 MeV
E*= 4 0 0MeV
T= 2MeV
E*= 17 8MeV
T= 4MeV
E*= 6 7 0MeV
Dipole strength (fm²)
ω (MeV)

Fig.15

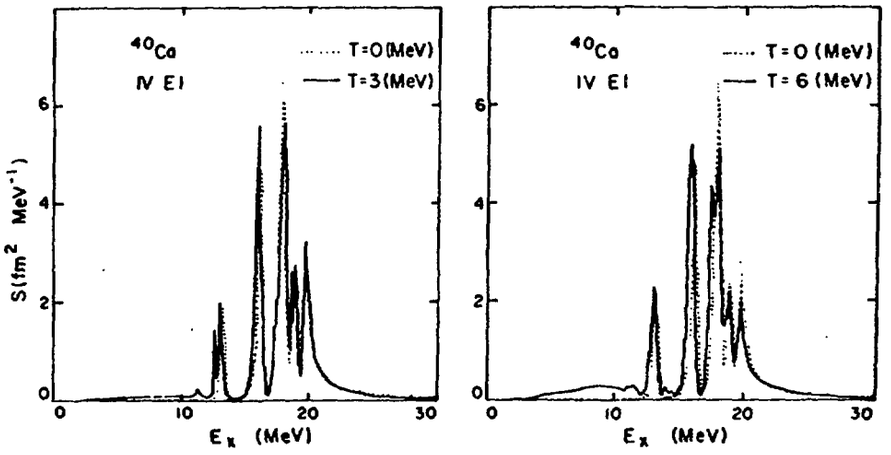
40Ca
IV E1
T=0(MeV)
T=3(MeV)
T=6 (MeV)
S(fm² MeV⁻¹)
Ex (MeV)

Fig.16

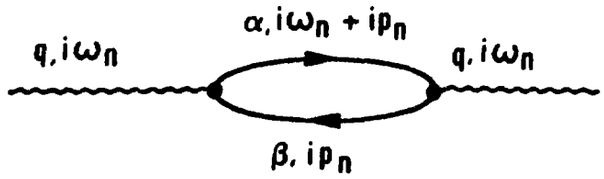

Fig.17

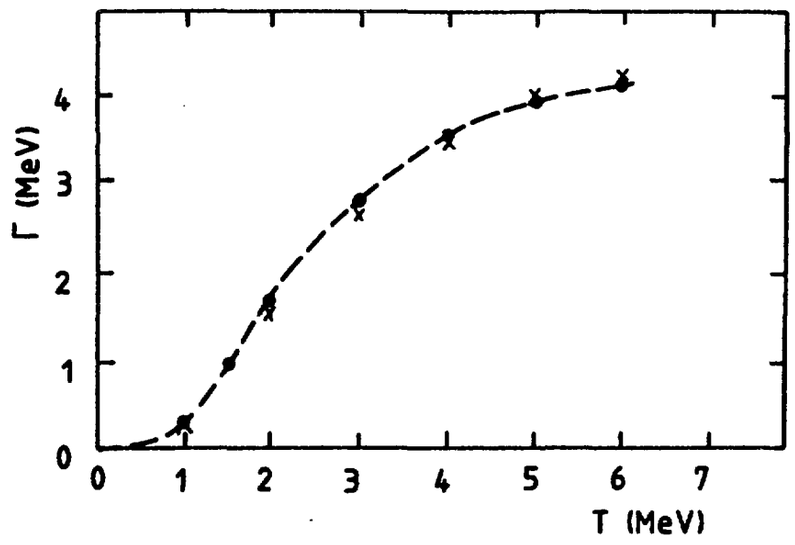

Fig.18

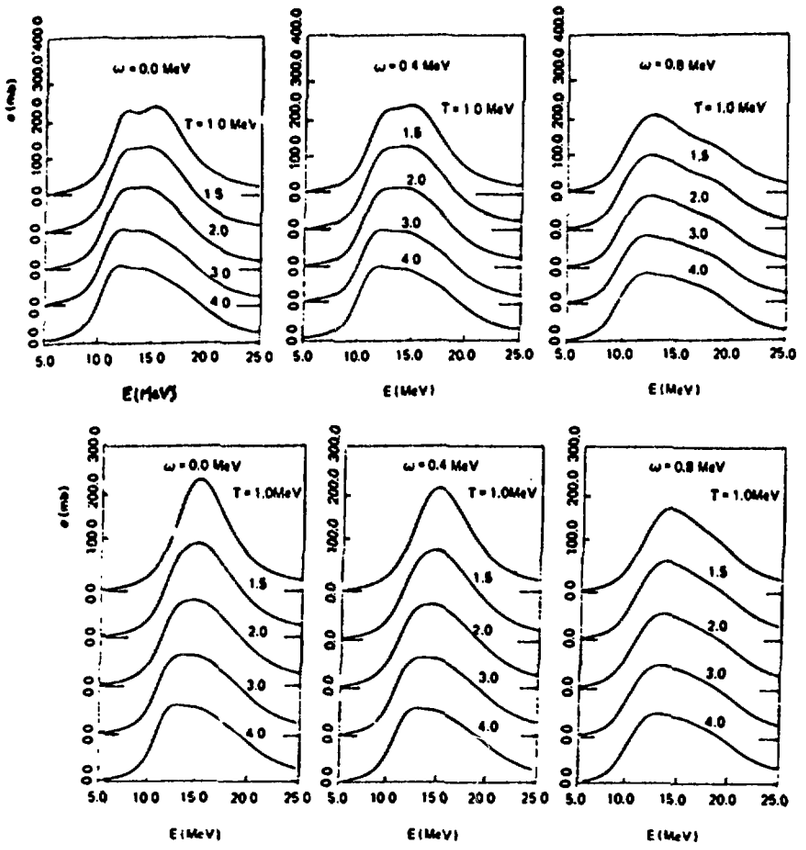

Fig.19

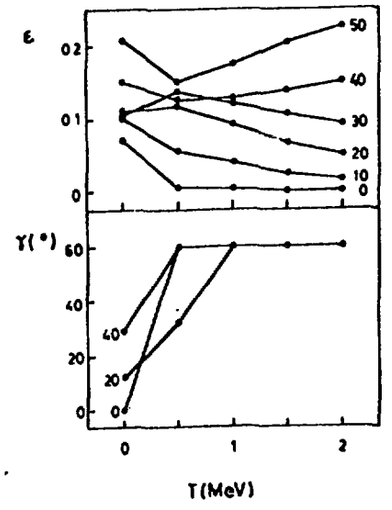

Fig.20